



Analysis of deuterium in V–Fe5at.% film by atom probe tomography (APT)

R. Gemma^{a,*}, T. Al-Kassab^b, R. Kirchheim^a, A. Pundt^a

^a Institute of Material Physics, University of Göttingen Friedrich-Hund-Platz 1, D-37077 Göttingen, Germany

^b Division of Physical Sci. & Eng., King Abdullah University of Science & Technology (KAUST) Thuwal 23955-6900, Saudi Arabia

ARTICLE INFO

Article history:

Received 30 July 2010

Received in revised form 6 November 2010

Accepted 17 November 2010

Available online 25 November 2010

Keywords:

Atom probe
Hydrogen
Deuterium
Vanadium
Thin film

ABSTRACT

V–Fe5at.% 2 and 10-nm thick single layered films were prepared by ion beam sputtering on W substrate. They were loaded with D from gas phase at 0.2 Pa and at 1 Pa, respectively. Both lateral and depth D distribution of these films was investigated in detail by atom probe tomography. The results of analysis are in good agreement between the average deuterium concentration and the value, expected from electromotive force measurement on a similar flat film. An enrichment of deuterium at the V/W interface was observed for both films. The origin of this D-accumulation was discussed in respect to electron transfer, mechanical stress and misfit dislocations.

© 2010 Elsevier B.V. All rights reserved.

1. Introduction

Recently, atom probe tomography (APT) [1,2] has opened up a new quantitative approach to trace hydrogen in metals [3–6]. In hydrogen-metal systems, the investigation of properties of hydride in reduced dimension has been one of the important issues for the development of hydrogen storage [7–9] and sensor application [10]. Moreover, direct observations of the local chemistry associated with this distribution of hydrogen at dislocations or at grain boundaries would be of particular interest to establish a fundamental understanding of phenomena such as hydrogen embrittlement [11]. APT is a powerful tool for such purposes because of its high spatial resolution in the analysis direction (0.1 nm).

However, it is not so straightforward to detect hydrogen in metals accurately just by utilizing APT because of diffusion phenomena. Even at cryogenic temperatures as low as 50 K, an interstitially solved hydrogen atom in a metal is highly mobile and has diffusion coefficient of 10^{-9} cm²/s (≈ 360 μ m²/h) e.g. in vanadium [12]. As APT is a destructive analysis, there will be always newly created surfaces and hydrogen atoms diffuse towards these energetically more favorable surface sites during the analysis. To avoid such surface segregation, use of heavier isotopes like deuterium (D) instead of H is thus strongly recommended for APT. In addition, D can be ultimately distinguished from residual hydrogen in the analysis chamber. Nevertheless, special care still must be taken for ana-

lyzing D quantitatively by considering the influence of analysis temperature on the diffusivity of D [4,5].

In this study, we have applied analysis temperature of 20–30 K in order to suppress surface segregation of deuterium. By this, a detailed picture of deuterium distribution in 2- and 10-nm thick V–5at.% Fe film was obtained as shown in the following sections. Regarding the obtained results, special attention is paid to the depth and lateral distribution of D atoms.

2. Experimental

The films were deposited on needle-shaped W substrate suitable for the APT analysis. The W tip substrate was sharpened by electropolishing and the surface was developed by field evaporation by the procedure described in [5]. The tips had a (1 1 0) orientation along the tip axis.

Deposition was carried out by ion beam sputtering, under Ar atmosphere at a pressure of 1×10^{-2} Pa, with deposition rates of 0.6 nm/min for V–Fe5at.% target. The base pressure of the sputtering chamber was in the range of $1-2 \times 10^{-8}$ Pa at room temperature. The deposition was carried out at 298 K. All of the films prepared were subsequently terminated by an approximately 5–10 nm-thick Pd layer, which promotes D₂ dissociation and protects V from oxidation as well.

Then the as-sputtered specimen was introduced into the deuterium-loading set up. The detailed loading process is described in [5]. This set up is equipped with a magnetic sample transfer rod which is coupled with a gate valve, so that the sample transfer from the loading chamber to the APT main chamber can be carried out without breaking the D₂ atmosphere. After reaching the base pressure of 10^{-5} Pa, the deuterium gas (purity: 99.98%) was leaked into the system at the desired pressure between 0.2 Pa and 1 Pa. After loading for 48 h, the transfer rod was removed from the set up and connected to a pre-evacuation chamber on the APT. Before introducing the sample into the main chamber, the remaining D₂ gas was removed. The APT analysis was carried out with a tomographic atom probe detector type [1] at 20–30 K with a voltage pulse fraction of 20% and a voltage pulse frequency of 2 kHz. The DC voltage of the sample changed typically from 3.5 kV to 15 kV to complete an analysis.

* Corresponding author. Tel.: +49 551 39 5025; fax: +49 551 39 5012.

E-mail address: rgemma@ump.gwdg.de (R. Gemma).

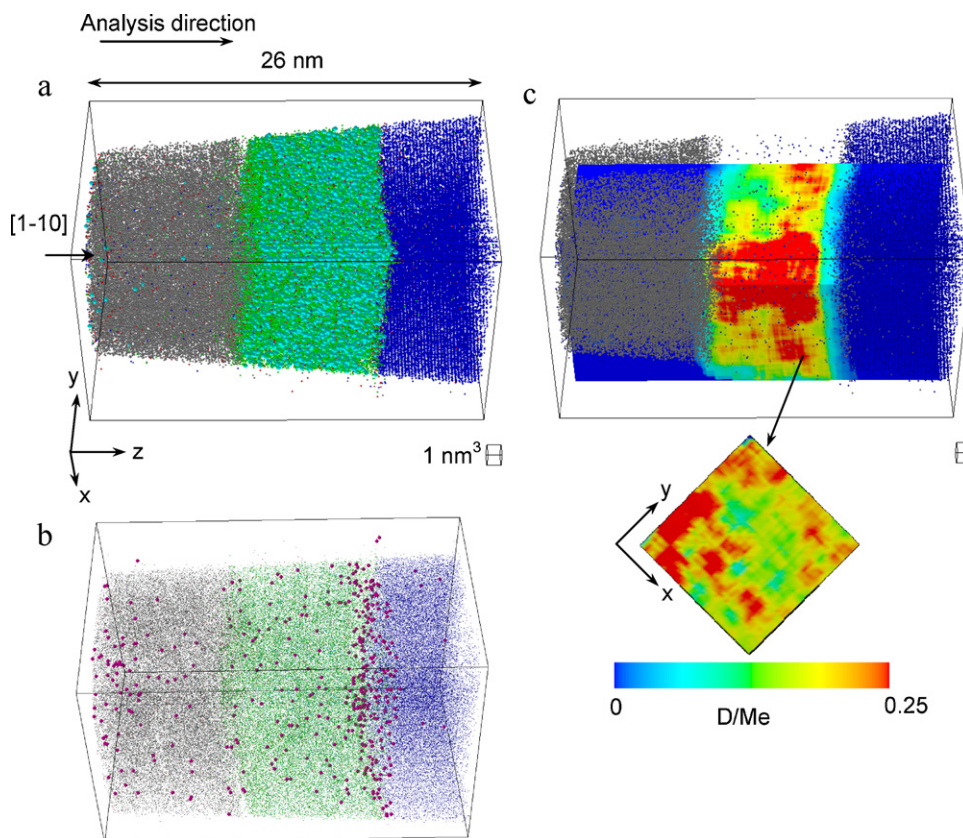


Fig. 1. Reconstructed volume from the analysis at 30 K ($13 \text{ nm} \times 13 \text{ nm} \times 26 \text{ nm}$), loaded with D_2 0.2 Pa. The small cube represents a 1 nm^3 box. (a) The whole volume of reconstruction (grey: Pd, green: V, red: Fe, blue: W, light blue: D). (b) Same reconstruction as (a), but with O (purple). (c) Iso-concentration map of D concentration from the same reconstruction in (a). Note high c_D near V/W interface. The xy plane at 13 nm is cut out and shown in (b). (For interpretation of the references to color in text, the reader is referred to the web version of the article.)

3. Results and discussion

Atomically resolved D-distributions in different V–Fe films are measured and carefully discussed in the following section.

Fig. 1(a) and (b) shows the result of an APT analysis carried out at 30 K on 10-nm thick film. This film was loaded with deuterium gas at 0.2 Pa at room temperature. At this pressure, an equilibrium concentration $c_D = 0.31 \text{ D/Me}$ is expected according to the corresponding p – c – T curve, which was recorded via electrochemical hydrogen loading of a similar film (not shown). The sample axis lies along $[1-10]$, so that an epitaxial relationship of the V(110) film plane with the (110) plane of the W substrate is identified. The reconstructed volume (Fig. 1(a)) shows higher number of D atoms (light blue spheres) in the V layer compared with that found in the Pd layer. No D-atoms are detected in the W-substrate. This observation is in agreement with the fact that the hydrogen solubility in Pd and in W at 294 K is 4 and 24 orders of magnitude smaller than that in V, respectively [13]. For W, therefore, the hydrogen solubility is negligible.

In Fig. 1(b) the distribution of oxygen (O) atoms (purple spheres) in the sample volume is shown. O atoms detected at the V/W interface were due to the exposure of the W substrate tip to air prior to deposition.

D-concentration analysis along low-indexed poles is not correct for quantification due to evaporation aberration effect [14]. This is shown in Fig. 1(c) where part of the sample volume is shown with iso-concentration maps of $\text{VD}_{0.25}$. The plotted iso-concentration planes (one zx and one zy plane) cross each other at the (011) pole. A D-enriched region with concentrations higher than 0.25 D/V is found all along the (011) pole. But, this has been

attributed to an evaporation aberration effect [14], which often occurs at crystallographic poles and does not imply an inhomogeneous D-distribution. D-atoms located at kink sites migrate via surface diffusion to the edge sites before evaporation and, thus, distort the D-position. This effect is significant at low-indexed planes. Therefore, such low-indexed pole regions are not useful for chemical composition analysis, since the APT concentration profile directly counts the number of atoms in a defined volume. The enrichment of D at the (011) pole was also noticed, even more significantly, at 45 K and 60 K (not shown). Considering the diffusion rate r of D atom in bulk V at 30 K, it is $4 \times 10^{-7} \text{ nm}^2/\text{h}$, is certainly smaller than the typical analysis speed of $\sim 5 \text{ nm/h}$. Therefore, D atoms keep their position in depth. But, surface diffusion can be orders of magnitudes larger, blurring the lateral D-positions in flat regions. Therefore, the region around the (011) pole was not sampled for all depth concentration profiles presented in this paper.

Additionally, the evaporation sequence can also be affected by local chemistry via modification of field evaporation strength E_F and sometimes it induces a significant deviation from the original position of atoms. In this case, special care must be taken by examining the interface of two different layers [15].

A characteristic feature in Fig. 1(c) is a dense, laterally spread D layer of about 2 nm thickness right at the V/W interface. This dense D volume is also shown as a 2-dimensional xy map. D is inhomogeneously distributed in the interface volume. In order to study the local chemistry at this interface, a cylinder with 5 nm diameter was placed away from the (011) pole and the concentration depth profile in the cylinder was calculated and shown in Fig. 2. The depth profile reveals that the D-distribution is not homogeneous: also in depth, there are deviations from the average D concentration of

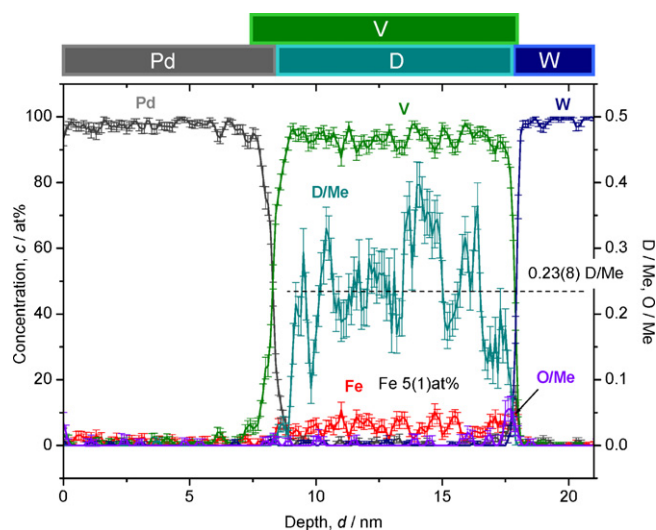


Fig. 2. Depth concentration profile taken from Fig. 1 (30 K). The average c_D in the V–Fe5at.% layer was in good agreement with expected, $c_D = 0.31$ D/Me. The error is indicated in the bracket. The error bars were calculated as $\sigma = [c(1-c)/(N-1)]^{-0.5}$, where c is concentration and N is number of detected ions. (For interpretation of the references to color in text, the reader is referred to the web version of the article.)

$c_D = 0.23(8)$ D/Me (the bracket indicates the error as standard deviation), especially at the depth of 12–13 nm, where $c_D = 0.4$ D/Me even exceeds the expected value of $c_D = 0.31$ D/Me. At such high concentrations, hydride precipitation is expected to occur in the bulk system. However, no hydride precipitates or clusters have been observed in this layered system. It was also confirmed by checking the correlation between Fe and D positions. As there is no significant modulation of the chemistry at the interface, the D-distribution at the V/W interface cannot be attributed to any evaporation aberrations. Thus, the enrichment of D near the V/W interface is a true result.

We suggest that the interface enrichment originates from defect-hydrogen interactions or from interface stress.

A similar analysis was carried out at 20 K, but with a D_2 loading pressure of 1 Pa, where an equilibrium concentration $c_D = 0.38$ D/Me is expected. At 20 K, the diffusion rate of D in bulk V is reduced to 9×10^{-4} nm/h [12], which is drastically lower than at

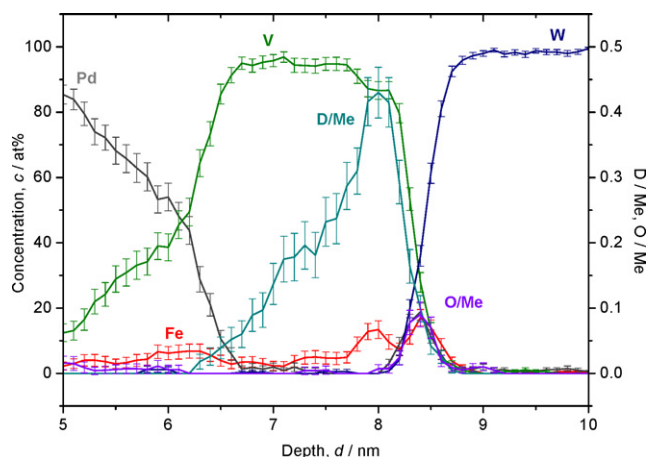


Fig. 4. Depth concentration profiles at the V/W interface. Note high c_{Fe} and c_D at V/W. The calculation of error bars is the same as in Fig. 2. (For interpretation of the references to color in text, the reader is referred to the web version of the article.)

30 K and more reliable analysis results were expected. But, unfortunately, the sample ductility was also reduced and, therefore, the sample was under the extreme risk of rupture caused by high voltage-induced mechanical stress during the APT measurement. Practically, successful results were only obtained for films with V layers thinner than 5 nm.

Results on a 2-nm thick V–5at.% Fe layer are shown in Fig. 3(a) and (b). Oxygen (O) atoms (purple spheres) were detected as well as in the case of Fig. 1. A homogeneous lateral distribution of D can be confirmed by iso-concentration maps. But, a significant accumulation of D is, again, found at the V/W interface. This trend is more obvious in the depth concentration profile shown in Fig. 4. A concentration peak reaching $c_D = 0.43(4)$ D/Me is found right above the V/W interface. In the middle of the V layer the D-concentration abruptly drops down to below 0.2 D/Me. Such a large difference cannot be attributed to the artifacts caused by the APT method.

The average D-concentration in the V–5at.% Fe layer is $c_D = 0.20(12)$ D/Me which is lower than that of the 10-nm thick film. This finding could be due to an increase of the plateau slope and a narrowed miscibility gap often observed by film thickness reduction [3]. Thus, no direct comparison of the mean concentra-

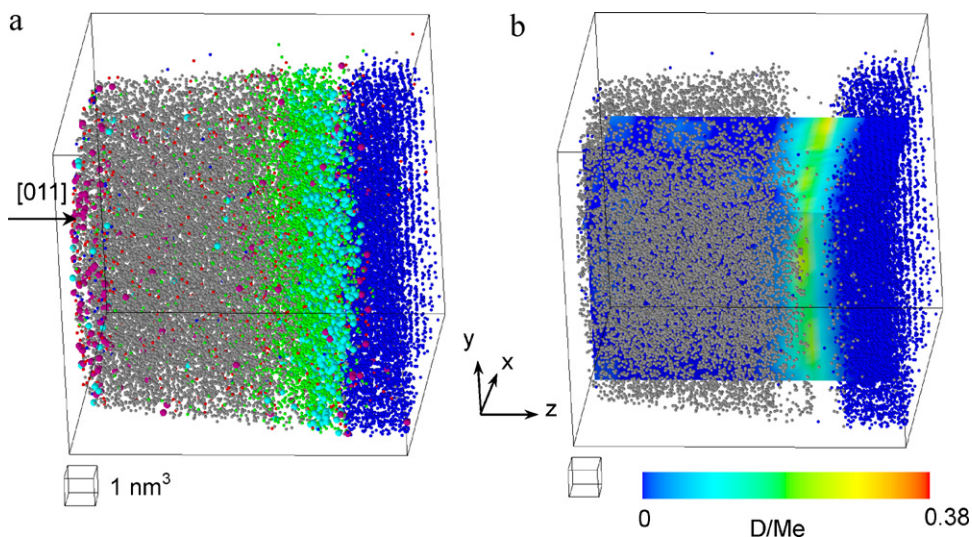


Fig. 3. The reconstructed volume from the analysis at 20 K (11 nm \times 11 nm \times 11 nm), loaded with D_2 at 1 Pa. (a) The whole volume of reconstruction (grey: Pd, green: V, red: Fe, blue: W, light blue: D, purple: O). (b) Iso-concentration map of D. Homogeneous lateral distribution of c_D can be confirmed. (For interpretation of the references to color in text, the reader is referred to the web version of the article.)

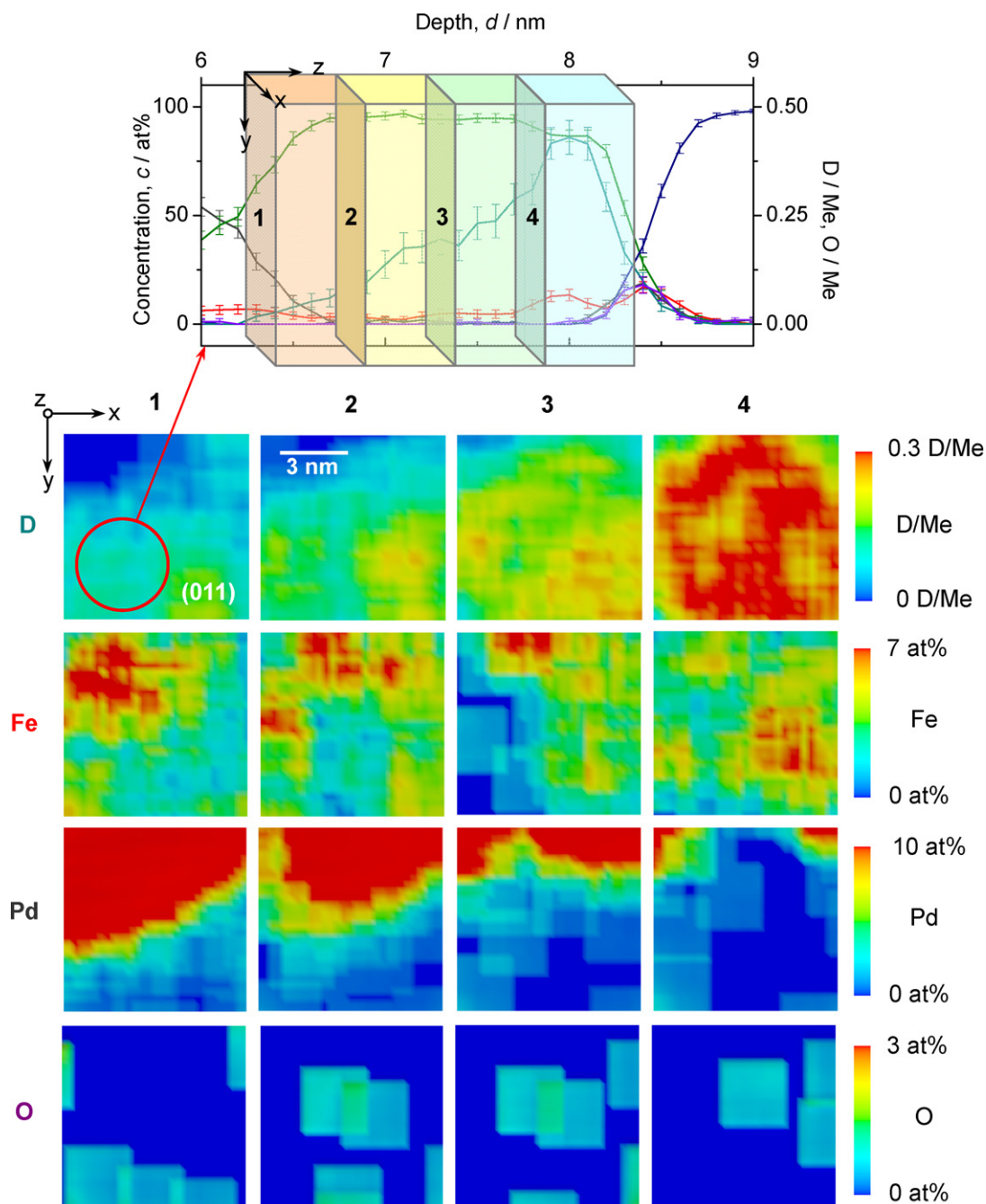


Fig. 5. 2d iso-concentration maps of D, Fe, Pd and O at each cross sectional depth (1–4). Each sampling volume ($3 \text{ nm} \times 3 \text{ nm} \times 0.5 \text{ nm}$) contains about 100 atoms. Red circle in the first image indicates the position of depth profiling. The position of the (0 1 1) pole is also shown. (For interpretation of the references to color in text, the reader is referred to the web version of the article.)

tion between the two samples is possible. Other notable features are (i) apparent intermixing of V and Pd at the surface, (ii) a lack of Pd at the maximum c_D peak and (iii) a little hump of Fe concentration profile at the same position as the maximum c_D peak. These features are examined in detail by applying 2d iso-concentration mapping of xy -volumes at different sample depths (1–4), as shown in Fig. 5. 2d maps of D, Fe, Pd and O at 4 depth positions are determined from the corresponding depth profile. The apparent intermixing of Pd with the V-layer (i) is simply explained by a tilt of the sharp Pd/V interface against the analysis direction, as can be deduced from the Pd- xy -maps clearly showing two distinct areas of Pd and V, each. The clear inverse concentration correla-

tion between the distribution of D and that of Pd (ii) can be also understood from the following point of view. In the xy -maps, the local concentration of D (1st row in Fig. 5) is low in Pd-rich regions (3rd row in Fig. 5). At the interface, local apparent “alloying” of V with Pd drastically decreases the D solubility [16]. This APT result reveals that even a small modulation of the local chemistry has a large impact on the D distribution of a reduced dimension at nm-range.

The correlation between D and Fe (iii) is not that straightforward as implied in the depth profile, though there are some overlaps barely seen especially in the 3rd and 4th columns. One should now focus on column 4, where a small dense region of Fe with about

17(2) at.% can be confirmed at the right-bottom. The other dense regions of Fe (in columns 1–3) can be ignored as they belong to the Pd layer. If the solubility limit of Fe in the V layer at room temperature is 12 at.% likely to that of bulk V [17], the excess Fe could have formed a second phase like σ -phase or its precursor. However, no cluster or platelet of Fe was found. Therefore, any strain field induced nucleation of deuteride at pre-existed precipitate can be discarded, concerning the volume analyzed.

For both V–Fe5at.% layers, an enrichment of D was detected at the film-substrate interface. The origin of this D accumulation is discussed in the following.

The dead-layer effects, suggested previously in Refs. [18,19] resulting from electron transfer at the interfaces of Fe/V and Mo/V system cannot explain the observed result at this V/W interface. The Fermi-level of electrons in W is much higher than in V, thereby resulting in an electron transfer towards the V layer. This electron transfer should decrease the local solubility of hydrogen at the V-side of the interface, which is opposite to the experimental finding.

Considering the impact of mechanical stress occurring at the interface of V and W, a cube-on-cube matching of V–5at.% Fe (with $a = 0.300$ nm) onto W (with $a = 0.317$ nm) results in 5.1% lattice mismatch. According to this, the V lattice is in a tensile strain state. Regarding the high stress sensitivity of the hydrogen site occupation in V [20,21], preferential formation of a D concentrated region caused by stress-induced site change at the V/W interface might explain the observed discontinuous D distribution. But, according to the model of Matthews and Blakeslee [22], the corresponding critical thickness for the implementation of misfit dislocations is 0.7 nm, for an ideal film.¹

Both analyzed films have thicknesses above the critical value and, thus, the presence of misfit dislocation is very likely. Since the V lattice constant is smaller than the W one, extra half planes are implemented in the V lattice. If the dislocation lines were located right at the interface (to accommodate maximum stress) compressive stress fields are expected above the V/W interface. D does not favor such regions. If the dislocation lines were located above the interface, D could be trapped there. This could, then, explain a deuterium segregation. But, the deuterium peak is located further away from the interface for the 2 nm V–5at.% Fe film. There, the c_D maximum is about 0.4 nm away from V/W interface. Taking a trapping region of 1–2 nm below the dislocation line into account [23] this would result in a further displacement of the dislocation line from the V/W interface.

Moreover, for both films, the presence of O atoms at the V/W interface can induce an enrichment of D atoms, due to large negative formation enthalpy of $D_2O(g)$ (249 kJ/mol at 298 K [24]). However, if D_2O were present, both peaks have to appear at the same sample depth, which was not the case. Therefore, we suggest that O was present as adsorbent and V is deposited on top of this. The thickness of natural W-oxide is about 3 monolayers [25] and the oxide does not grow at room temperature unless electronic field is applied [26]. It is likely that at certain positions at the V/W interface, nonstoichiometric V-oxide is formed. This precipitate does not absorb hydrogen, but due to its larger lattice constant than that of the V–Fe layer, misfit dislocations could be present above these precipitates. In the tensile strain field of these dislocations, deuterium could accumulate resulting in the observed c_D enrichments, simply also explaining the position of high c_D region

for both of the films. Additionally, the structural vacancies at the metal/metal-oxide interface induce irreversible hydrogen trapping [27]. The above mentioned microstructural aspects can be considered for the D enrichment at V/W interface.

One should also keep in mind a possible influence of mechanical stress induced by high electric field, which can reach as high as several GPa [28], on the D distribution. Moreover, the applied voltage, thus the surface stress changes with increasing the tip radius during analysis. In this study, the tip radius of the sample demonstrated in Figs. 1 and 3 was estimated to be 41 nm and 31 nm, respectively. Although we have observed nearly common feature for both of these samples, more detailed study focusing on such essential aspect should be one of the future subjects concerning analysis of deuterium in materials.

4. Conclusion

It was shown that APT analysis at low temperatures of 20–30 K can give reliable deuterium concentrations, when gas loading is performed without breaking the vacuum. This was exemplarily shown for two V–5at.% Fe films of 2- and 10-nm thickness deposited on a W substrate. In the analysis performed at 30 K, the film loaded with 0.2 Pa D_2 showed an average D concentration of $c_D = 0.23(8)$ D/Me, which was in good agreement with the expected concentration of $c_D = 0.31$ D/Me. It was demonstrated that low-indexed plane regions have to be excluded from the analysis for proper concentration determinations.

An enrichment of D was observed near the V/W interface which is explained by the presence of misfit dislocations.

References

- [1] T. Al-Kassab, H. Wollenberger, G. Schmitz, R. Kirchheim, Tomography by atom probe field ion microscopy, in: M. Rühle, F. Ernst (Eds.), High Resolution and Spectrometry of Materials, Springer Verlag, Berlin, 2002.
- [2] T.F. Kelly, M.K. Miller, Rev. Sci. Instr. 78 (2007) 031101.
- [3] A. Pundt, R. Kirchheim, Annu. Rev. Mater. Res. 36 (2006) 555–608.
- [4] P. Kesten, A. Pundt, G. Schmitz, M. Weisheit, H.U. Krebs, R. Kirchheim, J. Alloys Compd. 330–332 (2002) 225–228.
- [5] R. Gemma, T. Al-Kassab, R. Kirchheim, A. Pundt, Ultramicroscopy 109 (2009) 631–636.
- [6] J. Takahashi, K. Kawakami, Y. Kobayashi, T. Tarui, Scripta Mater. 63 (2010) 261–264.
- [7] L. Schlappbach, A. Züttel, Nature 414 (2001) 353–358.
- [8] H. Fujii, S. Orimo, Phys. B: Cond. Matter 328 (2003) 77–80.
- [9] V. Bérubé, G. Radtke, M. Dresselhaus, G. Chen, Int. J. Energy Res. 31 (2007) 637–663.
- [10] A. Baldi, G.K. Palsson, M. Gonzalez-Silveira, H. Schreuders, M. Slaman, J.H. Rector, G. Krishnan, B.J. Kooi, G.S. Walker, M.W. Fay, B. Hjörvarsson, R.J. Wijn-gaarden, B. Dam, R. Griessen, Phys. Rev. B 81 (2010) 224203.
- [11] H.K. Birnbaum, P. Sofronis, Mater. Sci. Eng. A 176 (1994) 191–202.
- [12] Zh. Qi, J. Völkl, R. Laesser, H. Wenzl, J. Phys. F 13 (1983) 2053–2062.
- [13] E. Fromm, E. Gebhardt, Gase und Kohlenstoff in Metallen, 26 of Reine und angewandte Metallkunde in Einzeldarstellungen, Springer-Verlag, Berlin/Heidelberg, 1976.
- [14] A.R. Waugh, E.D. Boyes, M.J. Southon, Surf. Sci. 61 (1976) 109–142.
- [15] E.A. Marquis, F. Vurpillot, Microsc. Microanal. 14 (2008) 561–570.
- [16] D. Artman, J.F. Lynch, T.B. Flanagan, J. Less-Common Met. 45 (1976) 215–228.
- [17] H. Landolt, et al., in: Arnold Eucken (Ed.), Landolt–Börnstein 5th Ed., Group 4, Springer Verlag, Berlin, 1950–1980.
- [18] B. Hjörvarsson, J. Ryden, E. Karlsson, J. Birch, J.E. Sundgren, Phys. Rev. B 43 (1991) 6440.
- [19] G. Andersson, B. Hjörvarsson, P. Isberg, Phys. Rev. B 55 (1997) 1774.
- [20] S. Koike, T. Suzuki, Acta Metall. 29 (1981) 553–565.
- [21] H. Sugimoto, J. Phys. Soc. Jpn. 53 (1984) 2592–2599.
- [22] J.W. Matthews, A.E. Blakeslee, J. Cryst. Growth 27 (1974) 118–125.
- [23] M. Maxelon, A. Pundt, W. Pyckhout-Hintzen, J. Barker, R. Kirchheim, Acta Mater. 49 (2001) 2625–2634.
- [24] M. Keddah, Electrochim. Acta 34 (1989) 995.
- [25] D.A. King, T.E. Maday, J.T. Yates Jr., J. Chem. Phys. 55 (1971) 3236.
- [26] C. Nowak, G. Schmitz, R. Kirchheim, Surf. Sci. 604 (2010) 641–648.
- [27] R. Kirchheim, A. Pundt, T. Al-Kassab, F. Wang, C. Kluthe, Z. Metallkunde 94 (2003) 3.
- [28] M.K. Miller, A. Cerezo, M.G. Heatherington, G.D.W. Smith, Atom Probe Field Ion Microscopy, Oxford University Press, Oxford, 1996.

¹ For the calculation of critical thickness, Burger's vector b (typically $a/2$ (1 1 1) for bcc structure), angle between the dislocation line and the Burger's vector α , angle between the slip direction and the direction which is perpendicular to the line of intersection of the slip plane and the interface $\lambda = 35.7^\circ$ and lattice mismatch f between the film and the substrate, are applied.